


RESEARCH ARTICLE

Impact of α -synuclein spreading on the nigrostriatal dopaminergic pathway depends on the onset of the pathology

Fanfan Sun^{1,2} | Armando G. Salinas³ | Severin Filser^{4,5} | Sonja Blumenstock^{1,2,4,6} | Jose Medina-Luque^{1,2} | Jochen Herms^{1,2,4} | Carmelo Sgobio^{1,2} 

¹German Center for Neurodegenerative Diseases (DZNE), Munich, Germany

²Center for Neuropathology and Prion Research, Ludwig-Maximilians University Munich, Munich, Germany

³Department of Pharmacology, Toxicology, and Neuroscience, Louisiana State University Health Sciences Center – Shreveport, Shreveport, Louisiana, USA

⁴Munich Cluster for Systems Neurology (SyNergy), Munich, Germany

⁵Institute for Stroke and Dementia Research, Munich University Hospital, Munich, Germany

⁶Molecular Neurodegeneration Research Group, Max Planck Institute of Neurobiology, Martinsried, Germany

Correspondence

Carmelo Sgobio and Jochen Herms, German Center for Neurodegenerative Diseases (DZNE), Munich 81377, Germany.
Email: carmelo.sgobio@med.unimuenchen.de (C. S.) and jochen.herms@med.unimuenchen.de (J. H.)

Funding information

Marie Skłodowska-Curie Innovative Training Network (MSCA-ITN), Grant/Award Number: SynDegen and EU Horizon 2020 AMD-721802-6; Munich Cluster for Systems Neurology - SyNergy, Grant/Award Number: EXC 2145 SyNergy – ID 390857198; China Scholarship Council, Grant/Award Number: 201606170111

Abstract

Misfolded α -synuclein spreads along anatomically connected areas through the brain, prompting progressive neurodegeneration of the nigrostriatal pathway in Parkinson's disease. To investigate the impact of early stage seeding and spreading of misfolded α -synuclein along with the nigrostriatal pathway, we studied the pathophysiologic effect induced by a single acute α -synuclein preformed fibrils (PFFs) inoculation into the midbrain. Further, to model the progressive vulnerability that characterizes the dopamine (DA) neuron life span, we used two cohorts of mice with different ages: 2-month-old (young) and 5-month-old (adult) mice. Two months after α -synuclein PFFs injection, we found that striatal DA release decreased exclusively in adult mice. Adult DA neurons showed an increased level of pathology spreading along with the nigrostriatal pathway accompanied with a lower volume of α -synuclein deposition in the midbrain, impaired neurotransmission, rigid DA terminal composition, and less microglial reactivity compared with young neurons. Notably, preserved DA release and increased microglial coverage in the PFFs-seeded hemisphere coexist with decreased large-sized terminal density in young DA neurons. This suggests the presence of a targeted pruning mechanism that limits the detrimental effect of α -synuclein early spreading. This study suggests that the impact of the pathophysiology caused by misfolded α -synuclein spreading along the nigrostriatal pathway depends on the age of the DA network, reducing striatal DA release specifically in adult mice.

KEYWORDS

dopamine, neurotransmission, nigrostriatal pathway, PFFs, spreading, α -synuclein

Jochen Herms shared senior authorship.

This is an open access article under the terms of the Creative Commons Attribution-NonCommercial-NoDerivs License, which permits use and distribution in any medium, provided the original work is properly cited, the use is non-commercial and no modifications or adaptations are made.
© 2021 The Authors. *Brain Pathology* published by John Wiley & Sons Ltd on behalf of International Society of Neuropathology.

1 | INTRODUCTION

α -synucleinopathies are a group of progressive neurodegenerative disorders characterized by misfolded α -synuclein that can serve as a scaffold that recruits endogenous α -synuclein to form pathologic inclusions and spread throughout the nervous system [1]. It includes Parkinson's disease (PD), the most common movement disorder in the elderly population [2]. Differential vulnerability in α -synucleinopathies has been shown in several anatomic brain regions, and within each region, only distinct neural populations are functionally and/or structurally affected by the presence of the pathology [3]. In PD, for example, the formation of α -synuclein-positive cytoplasmatic inclusions, called Lewy bodies (LBs), is a widespread feature detectable in dopaminergic (DA) neurons in the midbrain. However, only a subpopulation of DA neurons located in the *Substantia Nigra pars compacta* (SNpc) suffers from massive neurodegeneration in PD, compared with neighboring DA cells in the ventral tegmental area (VTA).

The inoculation of α -synuclein preformed fibrils (PFFs) into human cell cultures and mouse brains has been used to model the recruitment of endogenous α -synuclein into misfolded and aggregated LBs-like structures [4–7]. Studies of the spatiotemporal development of the α -synuclein pathology show that only specific neuronal phenotypes are involved in the spreading process, whereas others are able to confine the α -synuclein aggregates at the somatic level and restrict the subsequent spreading of the pathology to other connected areas. In particular, catecholaminergic neurons are more prone to uptake and spread exogenous α -synuclein compared with glutamatergic and GABAergic neurons [8].

Among catecholaminergic neurons, DA neurons and their selective vulnerability is a crucial topic in PD research, as the reduced availability of DA in the striatum is responsible for most, if not all, motor symptoms in PD patients [9]. This DA neuron selective vulnerability may be due to augmented sensitivity to intrinsic and extrinsic factors. For example, DA neurons are highly vulnerable due to their peculiar intrinsic cellular properties: a high metabolic demand to sustain their extensive axonal processes and mitochondria along with their widespread unmyelinated axons. Interestingly, LBs are also present in normal-aged brains, and a gradual but moderate loss of DA neurons, and/or reduced level of striatal DA, can be also observed in both healthy animals and humans during their lifetime [10, 11]. Among important extrinsic factors linked to PD vulnerability, microglia reactivity has been considered a key player [12].

To investigate the impact of seeding and the subsequent spread of misfolded α -synuclein along the nigrostriatal pathway, we studied the pathophysiologic effect induced by acute PFFs seeding into the midbrain. To model the progressive vulnerability of the DA

neuron life span, we compare two cohorts of mice with different ages: 2-month old (young) and 5-month old (adult) mice.

2 | MATERIALS AND METHODS

2.1 | Animals

Heterozygous TH-IRES-Cre transgenic mice were used in this study [13]. Two independent cohorts of mice were investigated: 2-month-old mice (defined as “young” group) and 5-month-old mice (defined as “adult” group). Five mice per group, for a total of four groups (young mice 1-month postinoculation [m.p.i.], young mice 2–m.p.i., adult mice 1-m.p.i., young mice 2-m.p.i.), were used in each set of experiments, if not indicated otherwise (Figure S1A). All animals were housed in groups under pathogen-free conditions, with food and water provided ad libitum ($21 \pm 2^\circ\text{C}$, at 12/12 h light/dark cycle). All experiments were approved by the Bavarian government (Az 55.2-1-54-2532-214-2016) and performed according to the animal protection law.

2.2 | Preparation of preformed α -synuclein fibrils

The α -synuclein monomers and PFF materials were prepared as previously described [14–16]. Briefly, the recombinant wild-type mouse α -synuclein was expressed in BL21 (DE3) *Escherichia coli* using a pRK172 plasmid (kind gift of Kelvin Luk and Virginia Lee, University of Pennsylvania, USA). BL21 (DE3) *E. coli* (Invitrogen, MA, USA) were transformed with the plasmid, and expression was induced with isopropyl- β -D-thiogalactopyranose (IPTG, Peqlab, Erlangen, Germany). Cells were lysed by boiling after heat inactivation of proteases. After centrifugation, the supernatant was filtered through Filtropur S 0.2 filters (Sarstedt, Nümbrecht, Germany), loaded on a HiTrap Q HP anion exchange column (5 ml, GE Healthcare, Munich, Germany), and eluted with a linear 25–500 mM NaCl gradient. Synuclein-containing fractions were concentrated using VivaSpin 2-columns (Sartorius, Göttingen, Germany). The α -synuclein fraction was diluted to a concentration of 5 mg/ml in 50 mM Tris-HCl, pH = 7.0. After freezing in liquid nitrogen, the protein was stored at -80°C .

PFFs were assembled from purified α -synuclein monomers (5 mg/ml) by incubation at 37°C and centrifugation at 1400 rpm for 96 h and stored at -80°C [17, 18]. Directly before injection, an aliquot of PFFs was sonicated four times with a handheld probe (SonoPuls Mini 20, MS1.5, Bandelin, Berlin, Germany) according to the following protocol: amplitude 30%, time 15 s (pulse on 3 s, pulse off 6 s).

2.3 | Stereotactic injection of preformed α -synuclein fibrils

Two- and five-month-old TH-IRES-Cre mice were anesthetized with ketamine/xylazine (0.13/0.01 mg/g body weight) (WDT/Bayer Health Care, Garbsen/Leverkusen, Germany). In anesthesia mice were injected with 1 μ l (5 μ g) of PFFs into the SNpc (coordinates relative to Bregma: -3.0 mm anterior, +1.5 mm lateral, +4.2 mm beneath the dura) [19] of the right hemisphere using a 5 μ l Hamilton syringe. Injections were performed at a speed of 100 nL/min with the needle left in place after injection for at least 5 min. The left hemisphere, as internal control, received 1 μ l sterile phosphate-buffered saline (PBS). To verify the injection coordinates, TH-IRES-Cre mice were also bilaterally injected with PFFs and sterile PBS mixed with AAV1.CAG.FLEX.tdTomato.WPRE.bGH (AllenInstitute864, titer 1×10^{13} vg/ml, dilution 1:10).

2.4 | Fast-scan cyclic voltammetry

Fast-scan cyclic voltammetry (FSCV) was used to investigate electrically evoked DA release in dorsolateral striatum *ex vivo*. Five TH-IRES-Cre mice from each of the experimental groups were analyzed, with the PBS-injected left hemisphere taken as an internal control for the PFFs-injected right hemisphere. Animals were sacrificed at 1 and 2 m.p.i. by cervical dislocation, and coronal brain slices (250 μ m) containing the dorsal striatum were prepared as described previously [20, 21]. Slices were kept in oxygenated modified Krebs's buffer as follows (in mM): NaCl 126, KCl 2.5, NaH_2PO_4 1.2, CaCl_2 2.4, MgCl_2 1.2, NaHCO_3 25, glucose 11, HEPES 20, L-ascorbic acid 0.4, at room temperature. For recordings, brain slices were kept at 32°C in a chamber perfused at a rate of 1.5 ml/min. Cylindrical carbon-fiber microelectrodes (50–100 μ m exposed fiber) were prepared with T650 fibers (7 μ m diameter, Goodfellow, Huntingdon, England) and sealed into a glass pipette. The carbon-fiber electrode was held at -0.4 V, and the potential was ramped to +1.2 V and back at 400 V/s every 100 ms. DA release was evoked by a rectangular, electrical pulse stimulation (if not specified otherwise: 400 μ A, 1.2 ms, monophasic) generated by a DS3 Constant Current Stimulator (Digitimer, Hertfordshire, UK). Electrical stimulations were applied every 4 min by a bipolar electrode placed in the *corpus callosum*. The recording electrode was placed at a distance of ~100 μ m from the stimulating electrode, within the dorsolateral striatum area. Data were collected using DEMON software [22]. Ten cyclic voltammograms of charging currents were recorded as a baseline before stimulation, and the average was subtracted from data collected during and after stimulation. Seeded/control part ratio of

DA peak amplitude responses was obtained from four to eight control-seeded paired recordings across the rostral-caudal extent of the dorsolateral striatum and averaged for each mouse. The slope time constant of the evoked DA response was used as an index of DA uptake. Two to four of the most representative control/seeded area pairs were chosen for studying the kinetics for each mouse.

2.5 | Immunohistochemistry

Five mice per group were sacrificed by transcardial perfusion at each time point, first with PBS followed by 4% PFA (w/v) in deep ketamine/xylazine anesthesia. Brains were removed and postfixed in PBS containing 4% PFA overnight before cutting 50- μ m-thick coronal sections with a vibratome (VT 1000 S from Leica, Wetzlar, Germany). Floating sections were permeabilized with 2% Triton X-100 in PBS overnight at room temperature and blocked with 5% normal goat serum (Sigma Aldrich) and 4% BSA (bovine serum albumin, VWR) for 6 h on a shaker at room temperature. Primary antibodies (anti- α -synuclein-phospho-S129, rabbit polyclonal, Abcam, Cambridge, UK; anti-Tyrosine Hydroxylase, mouse monoclonal, Merck, Millipore, Darmstadt, Germany; anti-IBA1, Guinea Pig polyclonal, SYSY, Goettingen, Germany) were incubated for 48 h at 4°C. Slices were washed 3×10 min with PBS and then incubated with the secondary antibodies (goat anti-rabbit Alexa Fluor 488, goat anti-mouse Alexa Fluor 568, goat anti-guinea pig Alexa Fluor 647 Invitrogen, Life Technologies GmbH) overnight at 4°C. After 3×10 min washing in PBS, sections were finally washed for 3×10 min with PBS before mounting them on glass coverslips with Dako fluorescence conserving medium (Dako, Hamburg, Germany). The concentration used for all the antibodies was 1:500.

2.6 | Confocal microscopy

Images were acquired by using an LSM 780 microscope. Laser wavelengths used for excitation and collection range of emitted signals were as follows: Alexa fluor[®] 48–488 nm/500–550 nm; Alexa fluor[®] 568–568 nm/578–603 nm; Alexa fluor[®] 647–633 nm/long pass 670 nm, under a 40X oil objective (Plan-Apochromat 40x/1.4 oil DIC). For imaging of the midbrain, 3-dimensional 16-bit image stacks of $1024 \times 1024 \times 12$ pixels tile (each tile: $212.34 \times 212.34 \times 12$ μ m) scans were acquired for the whole SNpc area of each hemisphere. For imaging of the striatum, three consecutively different positions along the dorsolateral striatum were acquired in each hemisphere as 3-dimensional 16-bit image stacks with a resolution of $1024 \times 1024 \times 12$ pixels (each tile: $212.34 \times 212.34 \times 12$ μ m).

2.7 | Stereology

For the quantification of TH-positive (TH⁺) neurons in SNpc, 3 brains from adult mice were collected 2 m.p.i., while Cavalieri estimator was used to estimate volume SNpc in both hemispheres. Brain sections outlines were carried out using a Zeiss fluorescent microscope (Imager.M2, ZEISS, Oberkochen, Germany) fully motorized and interfacing with a Dell computer running StereoInvestigator[®] (MBF Bioscience, Williston, Vermont, USA). SNpc cells labeled with corresponding markers were quantified in 8 serial coronal sections spaced 150 μm apart (section interval = 3), spanning the entire brain hemisphere. Outline and fiduciary marks were drawn at 2.5x magnification (EC-Plan-NEOFLUAR 2.5X/0.075, ZEISS, Oberkochen, Germany) to delineate reference points. Limits for areas of interest were drawn following a mouse brain atlas [23]. Cell counting was done blinded to genotype and treatment, at 63x magnification (Plan/APOCHROMAT 63X/1.4 Oil DIC, ZEISS, Oberkochen, Germany) using a 3D counting frame. See Table 1 for the parameters of stereological counting.

2.8 | Imaris image processing

The 12-image z-stacks acquired by confocal microscopy were used to create detailed 3D surface reconstructions of TH⁺ DA somata and striatal terminals, IBA1⁺ microglia cells, and their processes as well as pS129⁺ α -synuclein aggregates. The image z-stacks were processed in Imaris software v9.3.1 (Oxford Instruments, Zurich, Switzerland) to display 3-color channel fluorescence in a 3D isometric view.

For processing the midbrain images, multiple tile acquisitions of the entire SNpc were analyzed from 3 different coronal slices (Bregma: -3.5, -3.1, and -2.7 μm) in each animal. The SNpc brain area (control and seeded side) was identified according to the Allen mouse brain atlas [19].

The SNpc region was manually selected based on the location of TH⁺ somata along with the image stack. For TH and IBA1 signals, the threshold intensity was defined by Imaris default parameters set on the PBS internal control hemisphere and applied to the corresponding PFFs-injected hemisphere. For the pS129 signal (used as a proxy signal for α -synuclein aggregates), the threshold intensity was set just above the detection of the background signal in the PBS internal control hemisphere

and applied to the entire slice. Only pS129⁺ particles with a volume above 2 μm^3 were included in this analysis.

For processing the striatal region, 3 different ROIs (212.34 \times 212.34 \times 12 μm) from 3 coronal slices (Bregma: 0.04, 0.64, and 1.24 μm) were analyzed for each animal, within the dorsolateral quadrant. TH⁺ corticostriatal fiber bundle areas were excluded from the analysis. Similar to the SNpc, threshold levels for the TH and IBA1 signal intensities in striatal images were determined on the internal control side, while the pS129 signal intensity threshold was based on the intensity value just above the background signal in the corresponding internal control side. Only pS129⁺ particles volume above 0.5 μm^3 and IBA1⁺ particles volume above 5 μm^3 were considered in this analysis. The final measurements include (i) the volume covered by the TH⁺, IBA1⁺, and pS129⁺ expressed as a proportion of the corresponding brain area (SNpc and striatum) sampled; (ii) the number of TH⁺ and pS129⁺ particles. 3D colocalization between different signals was processed with custom MATLAB scripts.

2.9 | Statistical analysis

Statistical comparisons were performed using Prism 8.4.2 (GraphPad Software, San Diego, CA, USA). For DA release data from FSCV, two-way ANOVA followed by the Bonferroni post hoc comparisons were used to compare the percentage of DA release in the seeded side normalized by the control side over different seeding times. For the assessment of intergroup differences at single time points when ANOVA interaction was not significant, Student's *t*-test (two-sided) or LSD Fisher's test was applied. Statistical comparison of data collected from histologic analysis (IMARIS) was performed using MANOVA within the same brain region (SNpc and striatum) with the following independent factors: treatment (between factor: control vs seeded side), age (between factor: young vs old), and, when shown, anteroposteriorly (within factor: 3 levels with different bregma values) or TH colocalization (TH⁺ vs TH⁻). The normality of the distribution was tested in each group using D'Agostino–Pearson *omni-bus* test. Values were calculated as the means between mice, each considered as the means of each 3 samples in SNpc and 12 samples in the striatum. For *t* tests, the variance between groups was tested (*F* test) and not found to be significantly different. Cumulative

SNpc	Counting frame	Sampling grid size	Coefficient of error (Gundersen), $m = 1$	Average cell counts/sampling site
<i>TH</i>				
Control	50 \times 50 \times 12 μm	130 \times 130 μm	0.12	1.08
Seeded	50 \times 50 \times 12 μm	130 \times 130 μm	0.11	0.98

TABLE 1 Parameters for stereologic TH⁺ cell counting in the SNpc

frequency distribution (CFD) for each mouse was calculated and averaged per group. Data are expressed as mean \pm SEM unless otherwise indicated, with $p < 0.05$ defining differences as statistically significant (* $p < 0.05$, ** $p < 0.01$, *** $p < 0.001$).

3 | RESULTS

3.1 | PFFs inoculation site in the nigrostriatal pathway confirmed by genetic labeling in midbrain and striatum

A single injection of recombinant α -synuclein PFFs into the wild-type mouse brain is already enough to trigger an LB-like pathology. We chose to use wild-type mouse α -synuclein PFFs because they are able to induce pathology in mice within weeks, whereas human α -synuclein requires months to trigger pathology [4, 24, 25]. α -synuclein strains derived from humans or mice can interfere with each other, mitigating aggregate formation if the injected exogenous α -synuclein is not from the same species as expressed in the host [24, 26].

To verify that PFFs or PBS were successfully injected into SNpc and to navigate the FSCV recording site in the striatum, we mixed AAV1.CAG.FLEX.tdTomato.WPRE.bGH (AAV-tdTomato) with the seeding material for the stereotactic injection (Figure 1A). Upon Cre-induced recombination, DA neurons in SNpc expressed the tdTomato fluorescent protein 1 m.p.i. (Figure 1B), indicating that the seeding material was taken up by SNpc neurons. Before conducting the FSCV recording at each time point, striatal slices were investigated under an epi-fluorescence stereoscope (Figure 1C,D). The TH terminals of the contralateral, as well as the ipsilateral sides in the striatum, were also successfully labeled, which allowed recording DA release in the tdTomato-positive dorsolateral striatum (Figure 1E). Note that the injection in the midbrain also targeted the mesocorticolimbic pathway; fluorescent labels in the ventral tegmental area (VTA) and *Nucleus Accumbens* (NAc) were apparent as well. Samples without a clear expression of tdTomato in the dorsolateral striatum were not used for data collection.

3.2 | Unilateral PFFs inoculation in SNpc affects ipsilateral striatal DA release in adult mice

Dysfunction of striatal DA release in both α -synuclein overexpressing and knockout animal models [27–29] has been shown, but it remains unclear how seeding of α -synuclein PFFs in the SNpc would affect the DA release in the striatum. Although there are studies exploring striatal DA contents with HPLC in seeding models [4], we used FSCV to study the DA neurotransmission

with a more sensitive temporal (subsecond) and spatial (in the dorsolateral striatum, the projecting site of SNpc neurons) resolution.

Thus, we investigated whether the ex vivo striatal DA release recorded by FSCV would change following PFFs inoculation in SNpc in young [30] and adult (5-month-old) mice, at 1 and 2 m.p.i., respectively. The results are presented as the percentage of DA release in the PFFs seeded side normalized to the PBS-injected internal control side (Figure 1F–K). In young mice, the striatal DA release was unchanged 1 and 2 m.p.i. (Figure 1J, left histogram pair: $p > 0.05$) compared with the internal control. In adult mice, DA release was unchanged 1 m.p.i. but displayed a remarkable decline at 2 m.p.i. compared with the control side (Figure 1J). The kinetic of DA uptake (slope time constant), strictly dependent on the DA transporter (DAT) activity, was comparable in both young and adult groups (Figure 1K).

3.3 | In adult DA neurons, unilateral PFFs inoculation led to low somatic α -synuclein deposition and higher spreading along the nigrostriatal DA pathway

To investigate the potential cause of the differential striatal DA release rates in young and adult mice, we analyzed the distribution of α -synuclein aggregates in SNpc and striatum, in both young and adult mice. First, we compared the volume covered by α -synuclein aggregates between hemispheres. Although DA terminals from the SNpc project mainly ipsilaterally, at least 1–3% of the DA fibers reaching the striatum originate from the contralateral SNpc [31, 32]. Within the time windows, we analyzed our samples, aggregates formed nearly exclusively in the hemisphere ipsilateral to the PFFs inoculation (Figure 2A–D), whereas aggregates in the contralateral hemisphere were rarely detected (Figure S1A–D). Moreover, the spreading of α -synuclein from the SNpc did not reach the motor cortex as well (Figure S2). These evidence validate the hemisphere injected with PBS as a valid internal control, allowing us to use the hemisphere contralateral to the PFFs injection to define the thresholds for our quantification and exclude experimental errors, interindividual variability, and experimenter bias from our result interpretation.

Pathologic α -synuclein aggregates developed and accumulated 1 m.p.i. in PFFs-injected midbrains of both young (Figure 2A) and adult mice (Figure 2B). However, α -synuclein deposition in SNpc was more pronounced in young compared with adult mice (Figure 3A,B). Compared with 1 m.p.i., the formation of aggregates 2 m.p.i. in SNpc increased even more in young (Figure 2C) but not in adult DA neurons (Figures 2D and 3C,D).

In the striatum, α -synuclein significantly accumulated more in adult mice, 1 m.p.i. (Figures 2A,B and 3A,B). This suggests that within the first month after

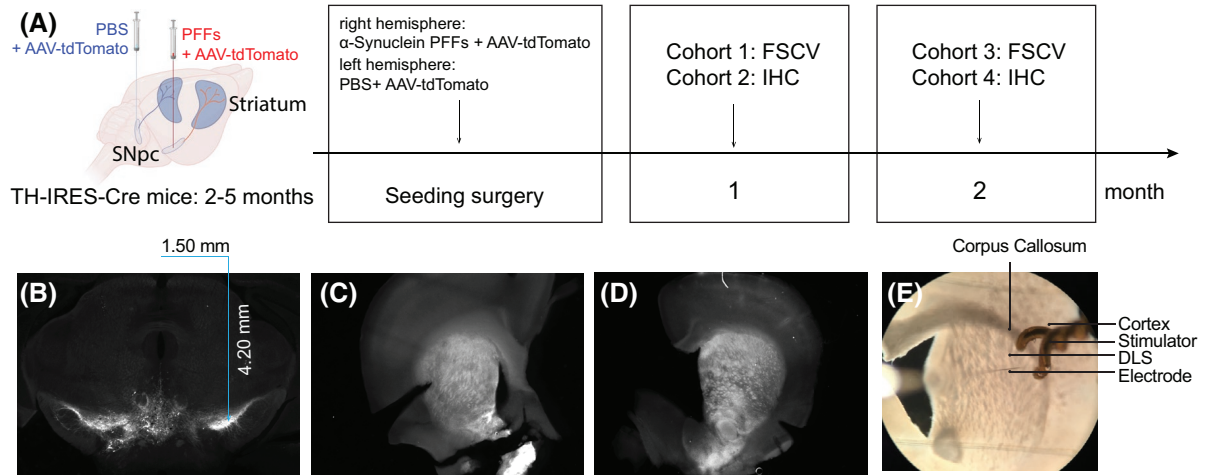
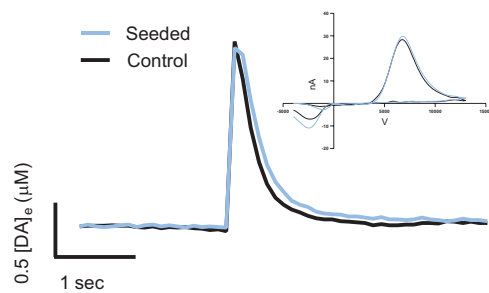
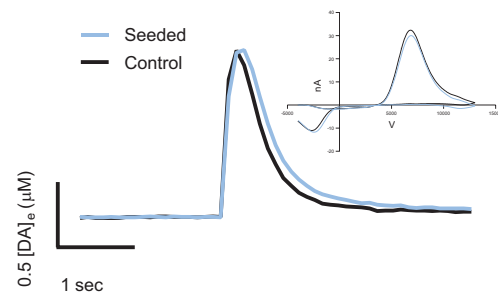
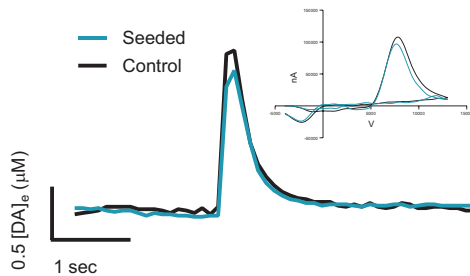
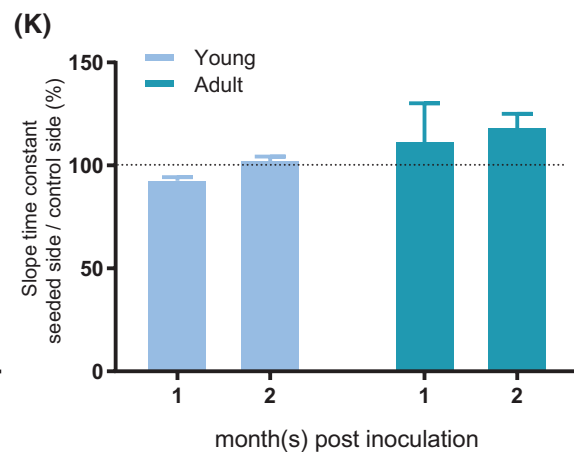
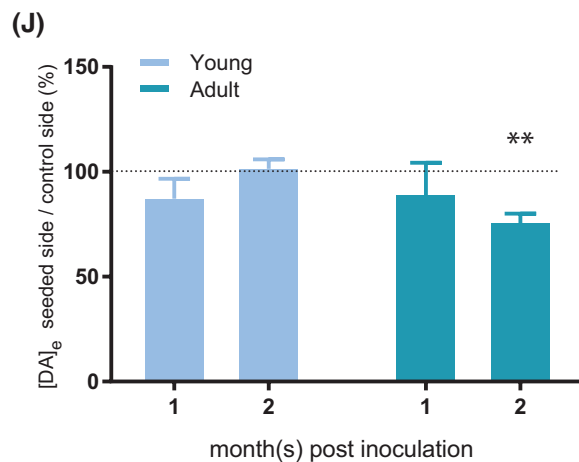
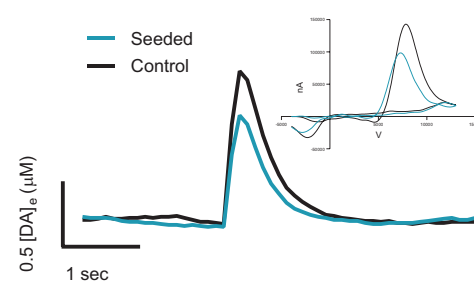
**(F)** Young (2-month-old) - 1 m.p.i.**(G)** Young (2-month-old) - 2 m.p.i.**(H)** Adult (5-month-old) - 1 m.p.i.**(I)** Adult (5-month-old) - 2 m.p.i.

FIGURE 1 Experimental inoculation of PFFs/or PBS/tdTomato reporter was validated for ex vivo electrically evoked striatal DA release. Experimental (A) scheme and expression of fluorescent tdTomato in the midbrain (B), in ex vivo striatal slice ipsilateral to the PFFs hemisphere (C, seeded side), and ipsilateral to PBS-injected hemisphere (D, control side). The FSCV setup and striatal recording site in the dorsolateral striatum (E). Representative traces of electrically evoked DA release with current/voltage (CV) curves in the insets in young mice (2-month-old) at 1 m.p.i. (F) and 2 m.p.i. (G) and adult mice (5-month-old) at 1 m.p.i. (H) and 2 m.p.i. (I). Evoked DA release ratio in seeded side normalized by their internal control side, at different postseeding time points in young and adult mice (J). Only in the adult mice, DA release shows a significant reduction ([DA]e: Control = 1.852 ± 0.2573 , Seeded = 1.424 ± 0.2448 , paired Student *t* test: $t(6) = 4.56$, $**p < 0.01$) 2 m.p.i. The slope time constant of DA uptake rate following the evoked release (K), expressed as the percentage in seeded side normalized by their internal control side, was not affected by PFFs inoculation ($p > 0.05$). $n = 5$ mice per group, 3–5 technical repetitions per hemisphere in each animal

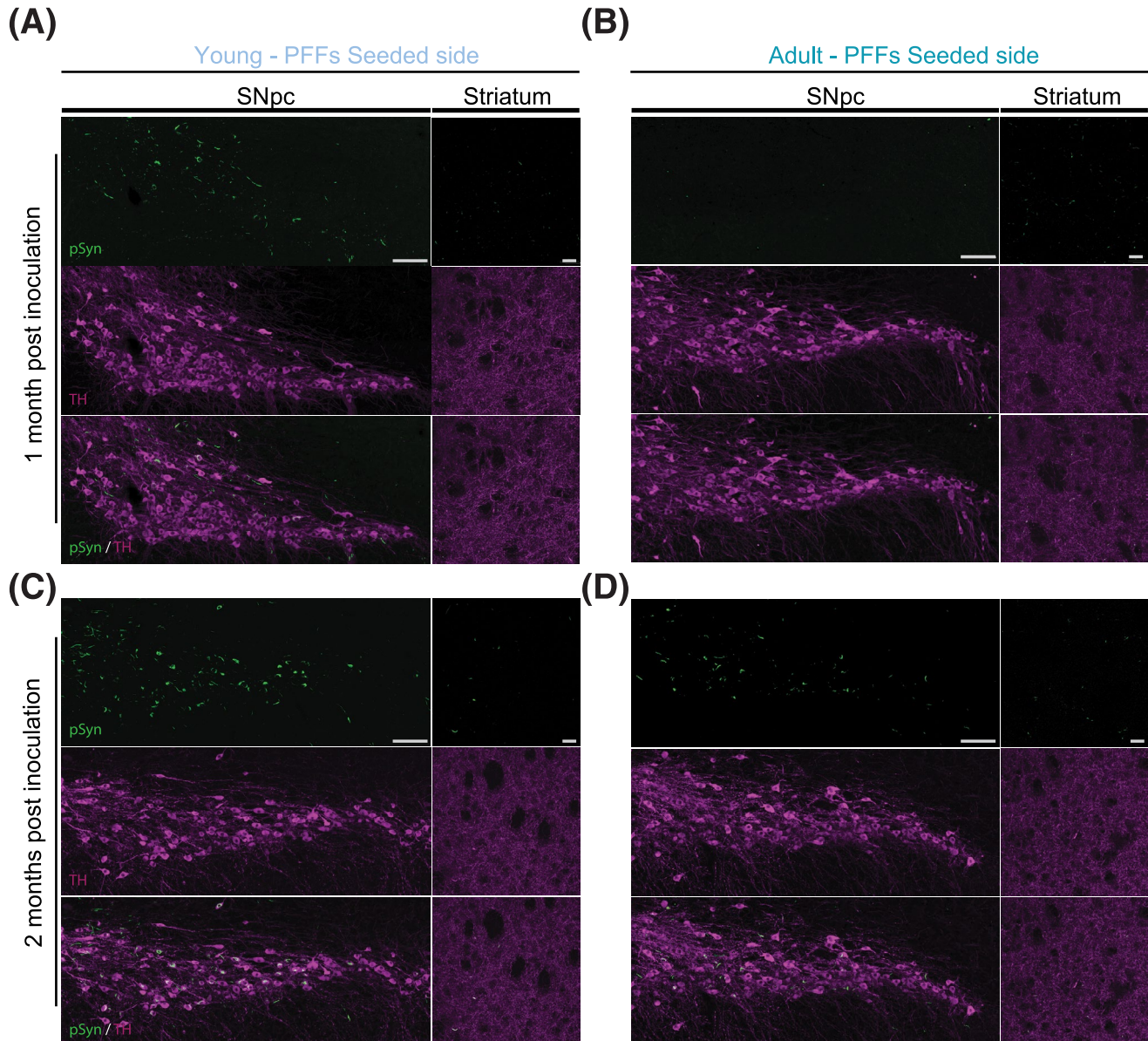


FIGURE 2 Representative images of immunohistochemistry staining in seeded SNpc and striatum of young and adult mice. Confocal acquisition of tile scanned SNpc reconstruction (left, scale bar: 100 μ m) and dorsolateral striatum (right, scale bar: 20 μ m) coronal area sections. Phospho- α -synuclein (pSyn) in green, Tyrosine Hydroxylase (TH) in magenta, and respective merged images. (A) Young and (B) adult brain areas, 1 m.p.i. (C) Young and (D) adult brain areas, 2 m.p.i.

inoculation, the spreading of α -synuclein pathology was significantly more pronounced in adults compared with what was observed in young DA terminals. The

distribution of aggregates in the striatum of young DA terminals did not change obviously from 1 to 2 m.p.i. (Figure 2C), instead, it decreased in adult DA

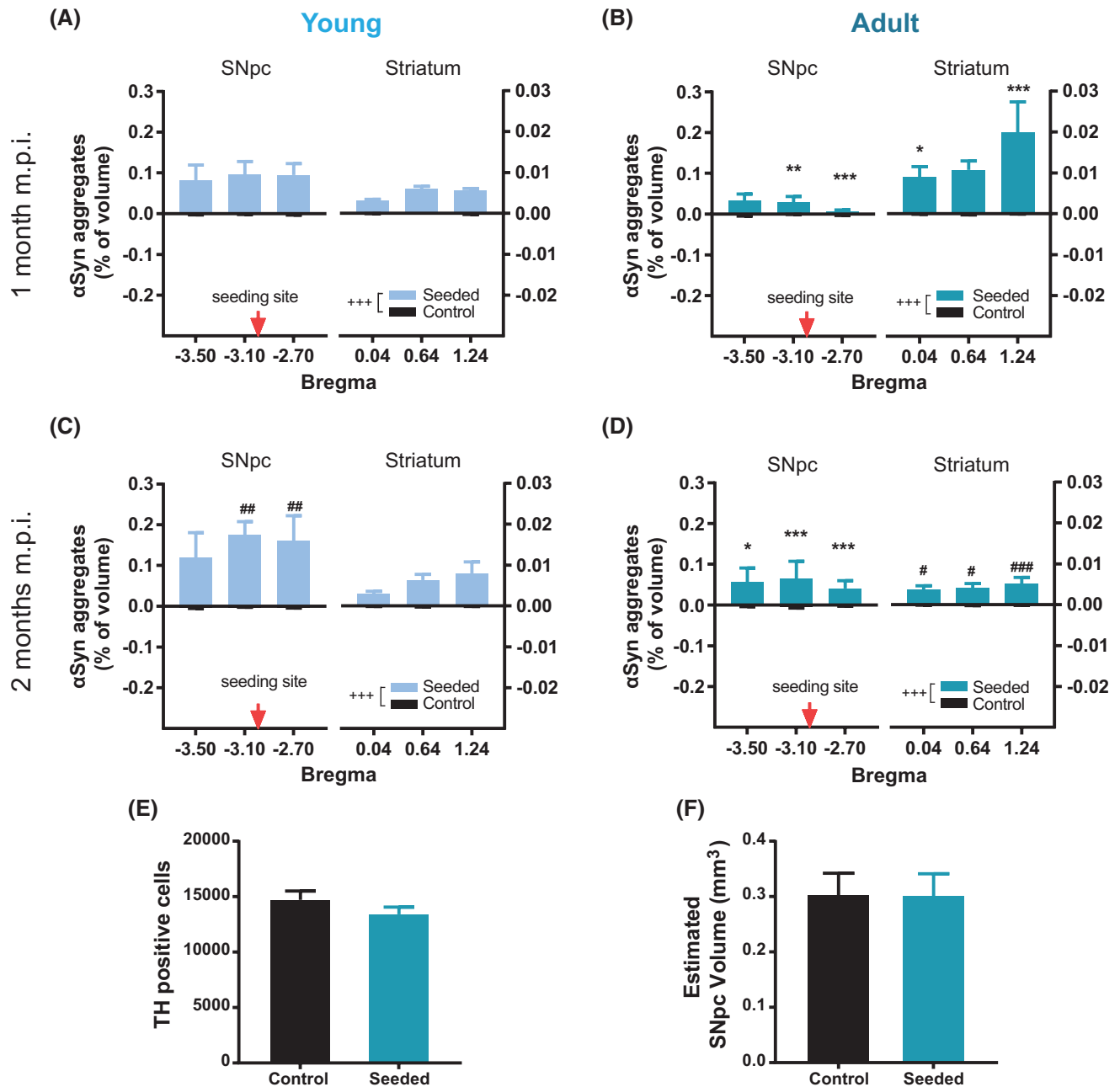


FIGURE 3 Distribution of α -synuclein aggregates from SNpc to striatum and stereologic counting of DA neurons. Volume covered by α -synuclein aggregates in SNpc and striatum in young mice at 1 m.p.i. (A) and 2 m.p.i. (B), and in adult mice at 1 m.p.i. (C) and 2 m.p.i. (D). Volumes covered by α -synuclein aggregates in the PFFs-injected hemisphere were always significantly higher than the respective contralateral PBS-injected sides (MANOVA Laterality Main Factor: $+++p < 0.001$). After 1 m.p.i., α -synuclein deposition in SNpc was more pronounced in young compared with adult mice, accumulating even more in young than in adult DA neurons at 2 m.p.i. (MANOVA significance in SNpc. Interaction treatment \times inoculation time: $F_{(1,1)} = 5.17$, $*p < 0.05$; interaction treatment \times age: $F_{(1,1)} = 16.41$, $***p < 0.001$). In the figures, LSD test: $##p < 0.01$ for comparison between different inoculation times of the same age; $**p < 0.01$, $***p < 0.001$ for comparison between different ages of the same inoculation time). In striatum, α -synuclein significantly accumulated more in adult compared with young mice, especially 1 m.p.i. (MANOVA significance in the striatum. Interaction treatment \times anteroposteriorly: $F_{(1,2)} = 5.26$, $*p < 0.01$; interaction treatment \times age: $F_{(1,1)} = 12.21$, $**p < 0.001$). In the figures, LSD test: $#p < 0.05$, $###p < 0.001$ for comparison between different inoculation times of the same age; $*p < 0.05$, $***p < 0.001$ for comparison between different age of the same inoculation time). $n = 5$ mice/group, 3 technical repetitions for SNpc, and 9 for striatum per hemisphere in each animal. Unbiased stereologic cell counting in adult mice at 2 m.p.i. (E) Estimated TH⁺ cells. (F) and estimated volume of SNpc in the seeded side and its internal control side. $n = 3$ mice per group

terminals to a level comparable with the one observed in young mice (Figure 2D) at 2 m.p.i. (Figure 3A–D). As suggested previously [8], the inclusion formation

after a single PFFs injection is likely to be transient in wild-type mice as healthy subjects are capable of eliminating the misfolded forms of α -synuclein pathology,

within tolerable levels of deposition. Our results highlight that this process can weaken with age. This can be a critical point where the physiologic adaptation may turn into pathology onset, especially when other factors are considered (genetic mutation, environmental stressors, etc.).

Besides, we also quantified the number of aggregates for each group (Figure S3). The number of aggregates in striata of young mice (Figure S3A) was significantly lower compared with adult mice (Figure S3B) 1 m.p.i. but not compared with 2 m.p.i. (Figure S3C,D). This suggests that adult brains accumulate less intracellular α -synuclein aggregates compared with young brains, leading to early prominent spreading of α -synuclein pathology from SNpc to the striatum.

To understand if the reduced striatal DA release in adult mice at 2 m.p.i. was caused by DA neuronal loss in SNpc, we further determined the number of TH⁺ DA neurons via unbiased stereologic quantification. Results showed that the number of TH⁺ DA neurons in the seeded side of SNpc was not significantly different from the control side (Figure 3E). The estimated SNpc volume (Figure 3F) was also statistically comparable between the seeded and the control sides.

Data from the colocalization analysis showed that phospho- α -synuclein (pSyn) positive aggregates mostly accumulated in TH⁺ neurons (Figure 4A). There were approximately 87% of aggregates located in the cell body and axons of TH⁺ neurons in the SNpc of young mice at 1 m.p.i., but 2 m.p.i. (Figure 4B) it increased to 92%. In adult mice, about 88% of the aggregates developed in TH⁺ structures in SNpc 1 m.p.i. and dropped to about 36% after 2 m.p.i. (Figure 4C), with a nonsignificant increase of overall aggregates volume.

In the striatum, the young group showed approximately 99% colocalization of aggregates and TH⁺ terminals 1 m.p.i. and around 92% after 2 m.p.i. (Figure 4D), with no significant change in overall aggregate volume. While in adult mice, the TH⁺ area colocalizing with aggregates was about 91% 1 m.p.i. (Figure 4E), which was slightly less than that in young mice. At 2 m.p.i., the TH⁺ area covered by aggregates was significantly reduced in adult mice, although with a similar colocalization of 92%, which was comparable with the level in young mice.

3.4 | In the striatum, the composition of TH⁺ terminals changed differently between young and adult DA innervation during α -synuclein spreading

We analyzed the volume covered by the TH⁺ terminals in the dorsolateral striatum in both young and adult mice. We found a nonsignificantly reduced TH⁺ axonal coverage in the striatum of young mice 1 m.p.i. (Figure 5A), whereas the reduction became significant after 2 m.p.i.

(Figure 5B). In adult mice, a nonsignificantly reduced TH⁺ axonal coverage (Figure 5C) was observed 1 m.p.i., but this trend did not reach significance even after 2 m.p.i. (Figure 5D).

To understand if the PFFs inoculation affected a specific population of terminals, we further compared the cumulative frequency distributions (CFD) of the size (μm^3) of the 3D reconstructed TH⁺ striatal terminals. The CFD was calculated per mouse and averaged for each group. In the young mice, the CFD curve of the ipsilateral seeded side was significantly left-shifted compared with the contralateral control side 1 and 2 m.p.i. This result indicates that the portion of small-sized terminals was always significantly higher in the hemisphere ipsilateral to the PFFs inoculation (Figure 5E) and also after 2 m.p.i. (Figure 5F).

However, adult mice displayed a different profile of the CFD pattern of TH⁺ terminals, which showed a smaller shift of significant differences of terminal size between the ipsilateral PFFs-injected side and the control side 1 m.p.i. (Figure 5G). While at 2 m.p.i., there was no significantly changed terminal distribution in adult mice (Figure 5H).

These results indicate that PFFs inoculation triggered modification in the striatal terminal density of young mice from 1 to 2 m.p.i., decreasing specifically large-sized terminals. Whereas, in the adult mice, this effect gradually disappears from 1 to 2 m.p.i.

3.5 | Coverage of microglia in the PFFs-seeded side showed reduced neuroinflammatory reactivity around adult DA terminals

To better understand the relationship between the seeding-induced alterations observed along the nigrostriatal pathway and the age-dependent microglial activation, we further quantified microglia coverage at each time point after PFFs inoculation in young and adult mice. In a previous pilot study, we did not observe any strong GFAP immunoreactivity in the SNpc or in the striatum, in either baseline and postseeding conditions (Figures S4 and S5). Likely, the reactivity of the microglia starts earlier than the astrogliosis, whereas astrocytic reactivity to α -synuclein spreading takes place later in the development of the pathology. Because we wanted to focus on the very early stage of the pathology spreading using the contralateral hemisphere as internal control, the role of astrocytes in the α -synuclein early stage of spreading would not be possible to investigate with our experimental design. Thus, we considered IBA1⁺ microglial coverage volume as a readout to evaluate the activation of microglia.

In young mice, the volume of microglial coverage in SNpc (Figure 6A) was always higher compared with the control side (Figure 6B). Considering the different patterns of aggregate formation observed in SNpc between

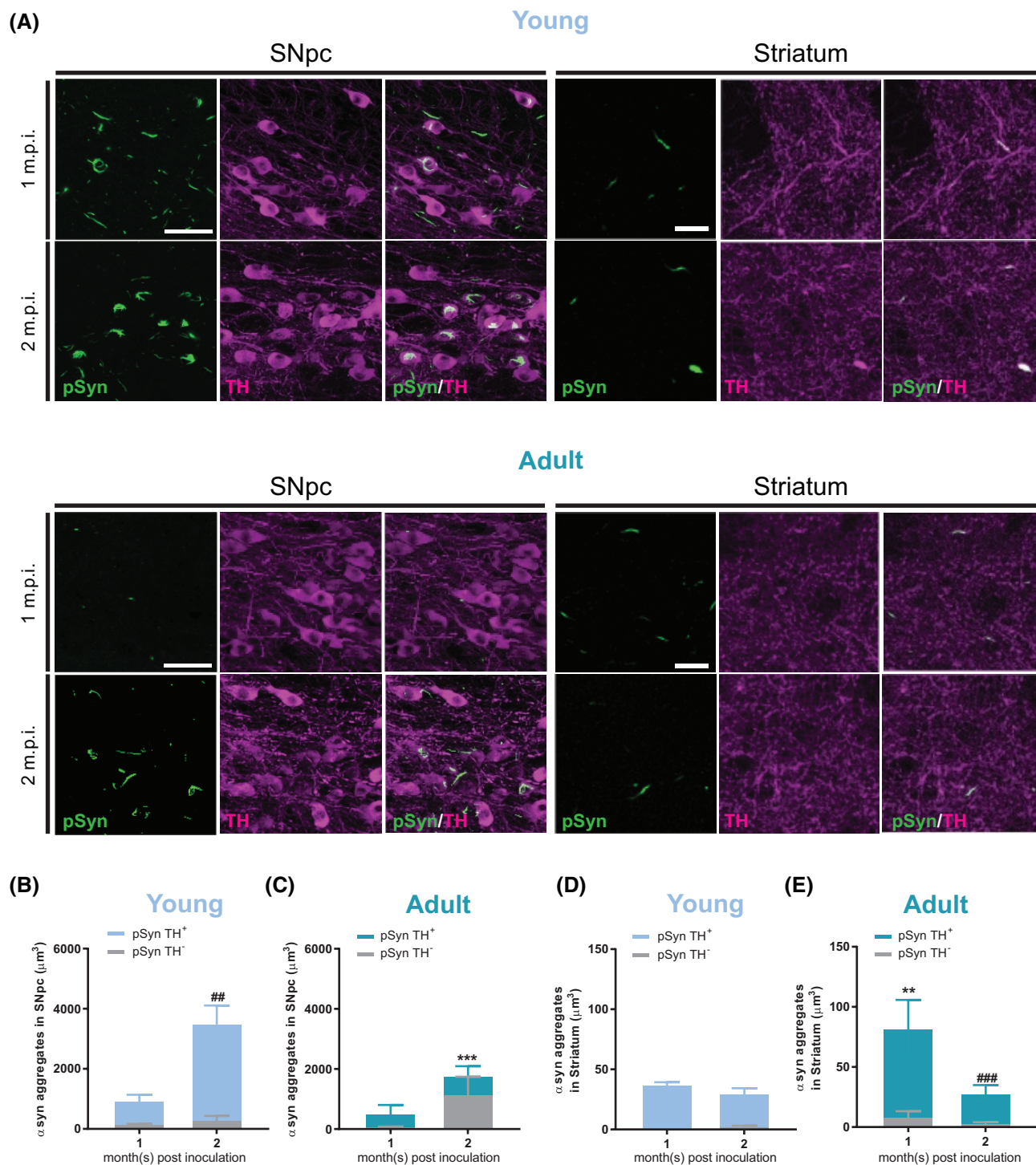


FIGURE 4 Colocalization of phospho- α -synuclein and Tyrosine Hydroxylase (TH) revealed different aggregate formations between young and adult DA neurons. Representative confocal images from SNpc (left) and dorsolateral striatum (right) areas of young (top) and adult (bottom) mice, 1 and 2 m.p.i. (A). Phospho- α -synuclein (pSyn) in green, TH in magenta and respective merged images. α -synuclein/TH colocalization in SNpc was $\sim 87\%$ and $\sim 92\%$ in young mice, from 1 to 2 m.p.i., respectively (B). In adult mice α -synuclein/TH colocalization in SNpc was $\sim 88\%$ and $\sim 36\%$ in young mice, from 1 to 2 m.p.i., respectively (C) (MANOVA significance in SNpc. Interaction Age \times TH Co-localization \times Seeding time: $F_{(1,1)} = 8.71$, $*p < 0.01$. In the figures, Bonferroni *post hoc* test: $##p < 0.01$, $###p < 0.001$ for comparison of aggregates in TH⁺ volume coverage between different inoculation of the same age; $***p < 0.001$ for comparison of aggregates in TH⁺ volume coverage between different age of same inoculation time). α -synuclein / TH co-localization in Striatum was $\sim 99\%$ and $\sim 92\%$ in young mice, from 1 to 2 m.p.i., respectively (D). In adult mice α -synuclein/TH colocalization in the striatum was $\sim 91\%$ and $\sim 92\%$ in young mice, from 1 to 2 m.p.i., respectively (E) (MANOVA significance in the striatum. Interaction TH Colocalization \times seeding time: $F_{(1,1)} = 4.37$, $p < 0.05$. In the figures, LSD test: $###p < 0.001$ for comparison of aggregates in TH⁺ volume coverage between different inoculation times of the same age; $**p < 0.01$ for comparison of aggregates in TH⁺ volume coverage between different ages of the same inoculation time). Scale bars: for SNpc, 100 μm ; for striatum, 20 μm . $n = 5$ mice per group, 3 technical repetitions for SNpc, and 9 for striatum per hemisphere in each animal

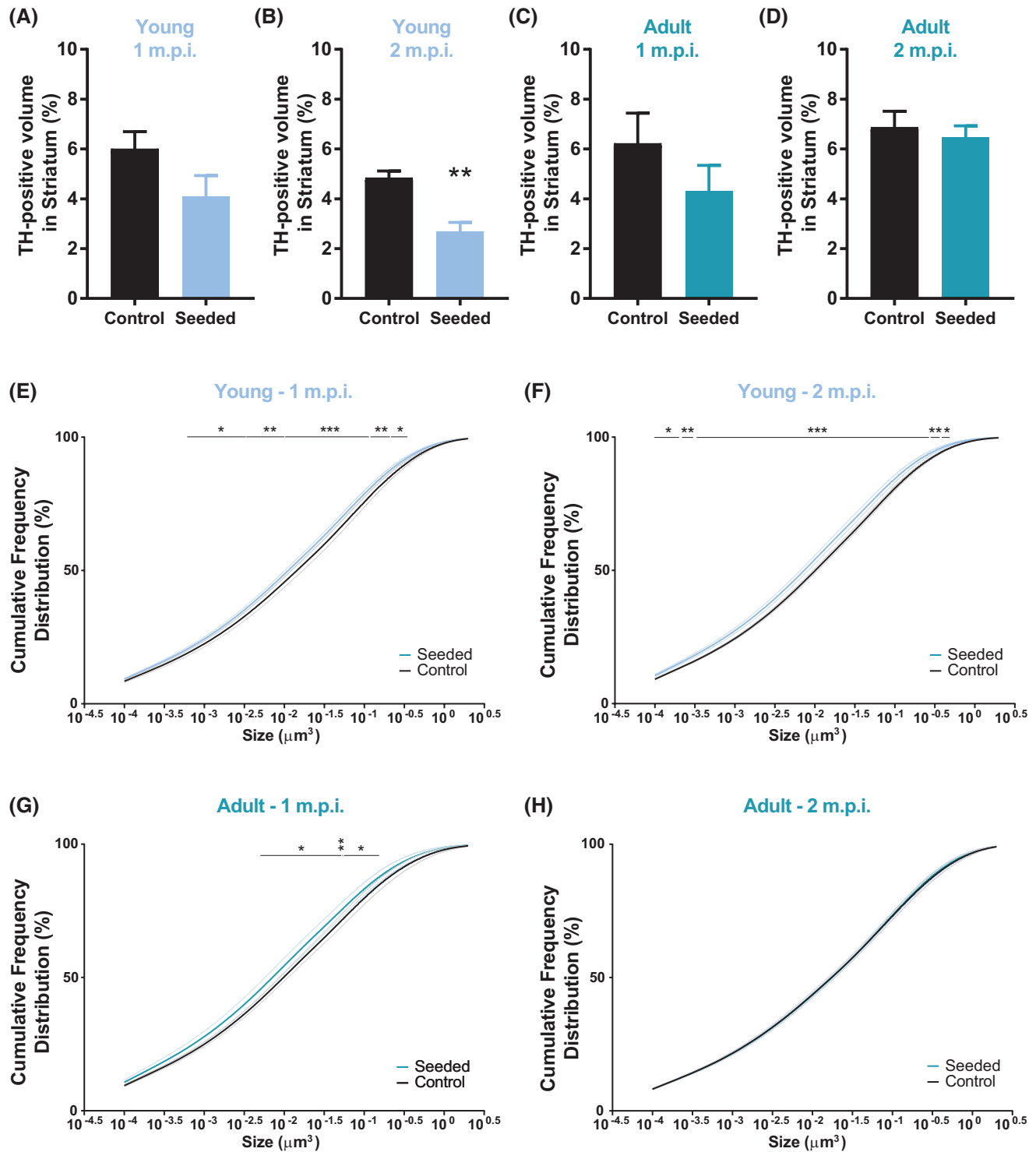


FIGURE 5 Striatal DA innervation modifies following PFFs inoculation in SNpc only in young DA neurons. Quantification of dorsolateral striatal volume covered by TH⁺ structures in young mice at 1 m.p.i. (A) and 2 m.p.i. (B), and adult mice at 1 m.p.i. (C) and 2 m.p.i. (D). In both groups, 1 m.p.i. revealed a nonsignificant trend of reduced DA innervation in the striatum ipsilateral to the inoculation. At 2 m.p.i., young mice showed a significant reduction of TH⁺ innervation, compared to adult mice where the innervation in the seeded hemisphere was comparable to the internal control hemisphere (unpaired *t* test $T_{(8)} = 4.199$, $^{**}p < 0.01$). The cumulative frequency distribution (CFD) curves were calculate per each mouse and averaged for each group (\pm SEM expressed with light color lines). CFD of TH⁺ terminal sizes showed significant left-shifted curves in the seeded side, revealing a higher proportion of small terminals in young striata at 1 (E, two-way ANOVA Main Factor Treatment $F_{(1, 160,008)} = 18,960$, $p < 0.001$; In the figure LSD test: $^{*}p < 0.05$, $^{**}p < 0.01$, $^{***}p < 0.001$) and 2 m.p.i. (F, two-way ANOVA Main Factor Treatment $F_{(1, 160,008)} = 38,852$, $p < 0.001$; In the figure LSD test: $^{*}p < 0.05$, $^{**}p < 0.01$, $^{***}p < 0.001$). In adult mice, CFD curves of TH⁺ terminal sizes in the seeded side were significantly left shifted at 1 m.p.i. (G, two-way ANOVA Main Factor Treatment $F_{(1, 160,008)} = 9780$, $p < 0.001$; in the figure LSD test: $^{*}p < 0.05$, $^{**}p < 0.01$) but not in adult striata at 2 m.p.i. (H, $p > 0.05$). No difference was detected between the seeded and internal control side. $n = 5$ mice per group, 3 technical repetitions for SNpc, and 9 for striatum per hemisphere in each animal

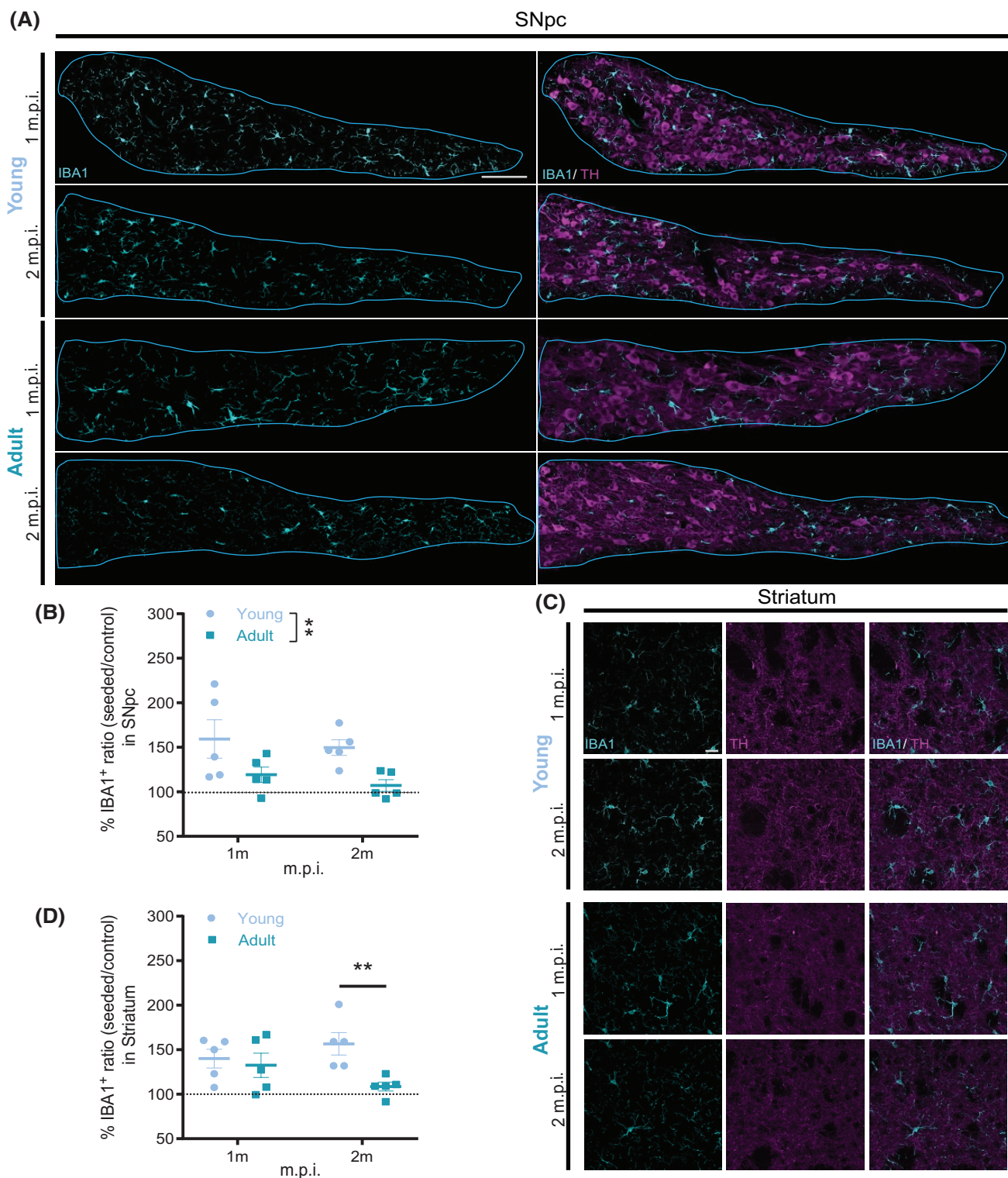


FIGURE 6 Microglial coverage volume increased in young mice, while adult mice showed limited microglial reactivity. (A) Representative images of IBA1 immunohistochemistry staining (left) and IBA1 merged with TH in SNpc in young (top rows) and adult (bottom rows) mice at different m.p.i. Scale bar: 100 μ m. (B) at 1 and 2 m.p.i. revealed a significantly higher IBA1 coverage in young mice (two-way ANOVA Main Factor Age $F_{(1,16)} = 6.366$; $*p < 0.05$). (C) Representative images of IBA1 and TH immunohistochemistry staining in the striatum of young (top rows) and adult (bottom rows) mice at different m.p.i. Scale bar: 20 μ m. Analysis of the microglia coverage volume in SNpc. In the striatum (D), the coverage volume of microglia in dorsolateral regions is higher in young compared with adult mice at 2 m.p.i. (two-way ANOVA Main Factor Age $F_{(1,16)} = 6.366$; $*p < 0.05$). Reactivity values are expressed as the ratio of microglia coverage volume in the seeded side normalized by each internal control side. $n = 5$ mice per group, 3 technical repetitions for SNpc, and 9 for striatum per hemisphere in each animal



young and adult mice, the high level of microglial activation coincided with the efficient formation of aggregates in young mice. While in adult mice, the lower level of activated microglia was accompanied by less α -synuclein deposition compared with young mice.

In the striatum (Figure 6C), the volume covered by microglia in young mice was constantly larger than the control side, which is similar to the phenomena in SNpc. While in the adult mice, the microglial coverage volume was increased at 1 m.p.i. and became comparable with its control side after 2 m.p.i. (Figure 6D). Notably, the high level of microglial coverage coincided with a decreased DA terminal density in young mice. While in the adult mice, lower coverage of microglia is associated with an unchanged DA terminal innervation.

4 | DISCUSSION

Our study aims to model the early presymptomatic stage of α -synuclein spreading, investigating the effects of acute PFFs seeding on α -synuclein pathology distribution, microglia reactivity, and neurotransmission associated with the nigrostriatal neurons. Our results showed a direct link between α -synuclein pathology spreading induced by seeding with reduced striatal DA release specifically in adult mice. Although α -synuclein pathology can affect a number of different neuronal populations in the brain, the mesostriatal DA neurons are critically important for the clinical development of PD. According to the Braak staging theory, the development of pathology does not follow a random pattern but, typically, the inclusions emerge with a topographical pattern which is classified as a six-stage progression [33]. In particular, stage 3 is characterized by Lewy body appearance in the midbrain before any occurrence in the cortex, and it is associated with the first appearance of motor symptoms.

At first, α -synuclein PFFs were inoculated into the midbrain and DA release was measured in the dorsolateral striatum. This area receives nigrostriatal afferents that are more sensitive to α -synuclein-dependent insults [34, 35]. Note that our FSCV studies were performed on striatal coronal slices where dopamine axons are functionally disconnected from the soma. Therefore, these results demonstrate that α -synuclein spreading toward DA axons affects neurotransmission at the terminals independently of any other changes in the DA neuronal activity due to the PFFs seeding. Interestingly, we found that electrically evoked DA release was significantly decreased by approximately 25% only in seeded adult striata 2 m.p.i., compared with their internal control side. The DA uptake rate in each group was similar to the internal control side.

Assuming the existence of a pathophysiologic phenotype in adult DA neurons, then we verified if α -synuclein pathology developed with different dynamics between adult and young DA neurons. First, we observed that

the amount of α -synuclein aggregates detected in the internal control side was always extremely low in each group at each time point. This indicates that at least after 2 m.p.i., the pathology was restricted to the hemisphere ipsilateral to the PFFs inoculation, which validates the contralateral hemisphere as a proper internal control.

We observed 1 m.p.i. in SNpc that phospho- α -synuclein positive aggregates already formed in the SNpc ipsilateral to the PFFs injection in both young and adult mice. However, according to our quantification, α -synuclein aggregates covered more volume in SNpc of young mice compared with adult mice. At the same time, we confirmed that the spreading of aggregates in the striatum was significantly elevated in adult DA neurons compared with the young ones. These results suggest that in young DA neurons, the misfolded α -synuclein proteins were more prone to accumulate into highly condensed somatic aggregates and propagate less to the striatum, compared with adult DA neurons.

At 2 m.p.i., we observed an increased accumulation of aggregates in the SNpc area, although it was significantly higher in young than in adult DA neurons. This result further supports the idea that pronounced α -synuclein deposition in SNpc is associated with a low propagation of the pathology into the striatum.

In the striatum, most of the α -synuclein aggregates were localized in the TH⁺ area, and never observed in the postsynaptic medium spiny neurons (MSNs) of the dorsolateral striatum. MSNs represent more than 95% of the neuronal population of the striatum and, as GABAergic neurons, they are mostly spared from developing Lewy body pathology [36–40]. Moreover, the absence of aggregates in the postsynaptic striatal neurons suggests that the spreading of α -synuclein in the first 2 months after PFFs seeding between midbrain and striatum was essentially anterograde. Therefore, we did not extend our investigation to the *Substantia Nigra pars reticulata*, where the majority of the striatonigral synapses reside [41].

In adult mice, the propagation of misfolded α -synuclein into striatum was significantly higher at 1 m.p.i. compared with the contralateral internal control, and eventually, it decreased after 2 months. It seems that the striatal neuronal network in seeded adult neurons was able to cope with the high spreading of aggregates from SNpc at 1 month, so the presence of aggregates cannot account for the decrease in DA neurotransmission but may function to protect the terminals from the increased concentration of harmful, soluble oligomers. In fact, α Syn may exist in different forms in neurons, from monomers to soluble multimers, and some forms of α Syn oligomers may be responsible for toxicity that affects presynaptic vesicle composition and release [42]. It has been shown that α -synuclein oligomers are able to decrease synapsin SYN1 and SYN2 gene expression, which in turn decreases two transcription factors, cAMP response element binding and Nurrl, that regulates synapsin gene promoter activity [43]. Moreover, transgenic

overexpression of α -synuclein oligomers in DA presynaptic terminals leads to enhanced age-dependent spreading pathology accompanied by behavioral abnormalities, reduced striatal DA content, and DA neuron loss [44]. Notably, these mice were monitored starting from 3 months and motor impairments were detected only between 14 and 24 months of age. Our findings are in accord with these prior studies showing a very early impact of the spreading α -synuclein pathology on the ability of striatal terminals to release DA. They also open the likelihood that early adaptive mechanisms might take place at the beginning of the spreading process and affect the evolution of the pathology.

Further, DA neurotransmission in young mice was not affected by the PFFs inoculation, and their preserved ability to release DA correlated with a constant, low density of striatal α -synuclein aggregates in the striatum.

In PD cases, as the disease progresses, neuronal or terminal loss usually accounts for the decreased DA neurotransmission in the striatum, which further contributes to the onset of motor dysfunctions. In adult mice 2 m.p.i., the total number of TH⁺ DA neurons in SNpc did not change significantly, implying that the decreased striatal DA release was not caused by neuronal loss in SNpc, which is consistent with previous results [25] but adds to the existing knowledge that α -synuclein-dependent early synaptic alterations precede neurodegeneration.

Surprisingly, when we analyzed the DA innervation in dorsolateral striatum, the volume covered by TH⁺ terminals significantly decreased in young mice, but not in the adults.

While the loss of DA innervation in the striatum is the principal cause of PD motor symptoms [45], early loss of neurons from SNpc is not directly associated with any clinical sign of the disease. Motor deficits in PD patients are evident only when at least ~50%–60% of DA neurons are lost [46]. The concept of “reserve” has been introduced to explain the mismatch between the degree of observed pathologic changes in the brain and their clinical manifestations. In PD, for example, neuronal and motor cognitive reserve were hypothesized to explain the individual's capacity to tolerate PD pathology, which can be maintained throughout disease progression [47, 48]. But this also implies the existence of compensatory mechanisms to counter the pathology development in preclinical and early stages of the disease. This is particularly true for PD because the unique properties of the nigrostriatal pathway guarantee high redundancy in their anatomic connections and activity [30]. For instance, dopaminergic axon arborization is not only dense in presynaptic boutons but also exceptionally large, so a single DA neuron is able to reach a large population of postsynaptic medium spiny neurons [49, 50]. Also, DA neurotransmission utilizes volumetric transmission [51, 52], so every glutamatergic postsynapse is always in close contact with a dopamine release site. The redundancy of the “boutons reserve” in the dopaminergic innervation is

also confirmed by the existence of functionally “silent” dopaminergic terminals [53], thus a heterogeneity of individual dopamine boutons that can diversify their activity in response to insults is likely. Several compensatory mechanisms are surely in place at the very early stage of PD, where axonal dying-back and compensatory sprouting compete with each other in order to preserve normal striatal physiology and eventually recover from different sources of damage. Those compensatory processes are hard to observe in PD patients, so insights gathered from animal models are especially valuable to elucidate the anatomic changes that occur in the very early stage of the α -synuclein pathology development.

After further analysis of the missing DA terminals in the young inoculated mice, we found that the portion of large-sized terminals was more likely to be affected by the spreading of α -synuclein pathology in young mice. Those terminals, defined by Gerfen and colleagues as “Type B,” characteristically belong to a specific DA neuronal subpopulation localized on the ventral tier of the SNpc [54] that are more prone to degenerate in PD patients although in mice they are resistant to PD-like insults [55]. It might be that Type B DA terminals represent the first line of defense against α -synuclein spreading, adding more knowledge on the possible diverse early compensatory processes occurring in the striatum. We suggest that selective pruning of inefficient DA terminals can also take place in healthy brains without eventual neuronal loss. Type B DA terminals might gather more misfolded α -synuclein within them in order to activate the neuroinflammatory response for efficient synaptic pruning. This process may be not as efficient in adults as in young DA neurons. Notably, type B DA terminals are also highly enriched with DAT [21]. In case of an inefficient microglial synaptic pruning, the persisting type B DA terminals would be affected by high α -synuclein spreading exposures. To corroborate this theory, we investigated whether the α -synuclein seeding had a distinctive microglia response to the spreading, depending on the maturation of the neurons.

After PFFs inoculation in SNpc, the microglial coverage volume in SNpc was increased in both young and adult seeded DA neurons compared with their non-seeded hemisphere, although it was significantly higher in young mice compared with adult mice. This suggests that the formation of aggregates potentially induces microglial activation, which in turn might constrain the α -synuclein spreading in an aggregated form inside the somatic compartment of young DA neurons.

In the striatum, the volume covered by microglia was higher in both young and adult mice compared with their internal control side at 1 m.p.i. More importantly, the coverage of activated microglia was significantly reduced in adult mice 2 m.p.i. but remained significantly higher in young mice. Although purely correlative, our results highlighted that sustained microglial coverage in striatum goes along with preserved DA release and

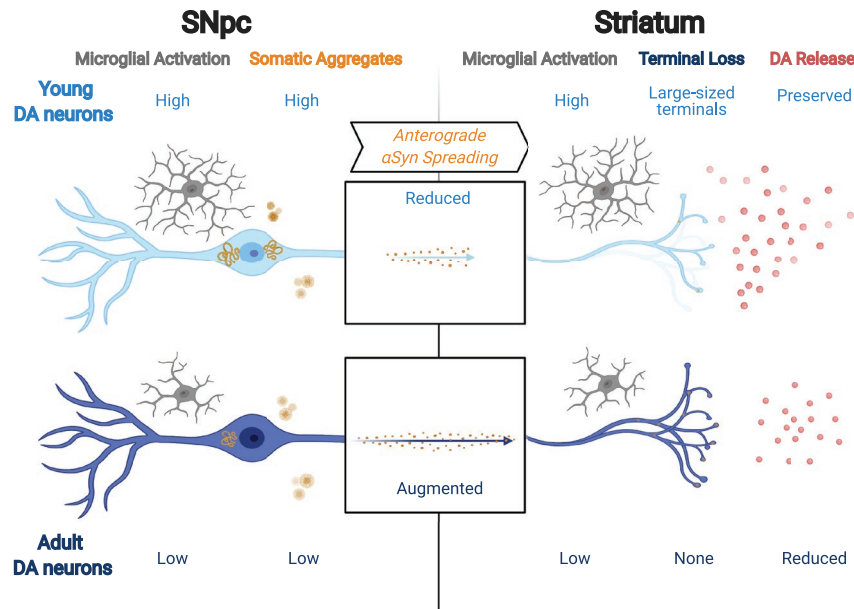


FIGURE 7 Interpretative model of changes over time in mouse SNpc PFFs model between young and adult DA neurons. α-synuclein PFFs in the nigrostriatal pathway cause aggregates and anterograde spread depending on the age of the DA neurons. Less somatic α-synuclein aggregates and augmented spreading pathology were observed in adult DA neurons compared with younger ones. Seeding nigrostriatal DA neurons in young DA neurons was associated with higher microglia coverage, large-sized (type B DA neuron) terminal loss, and preserved dopamine release, while seeding in adult DA neurons was associated with low reactive microglia, no terminal loss but reduced dopamine release. Created with BioRender.com

a reduced fraction of large-sized (type B) terminals. It has been also shown that aged microglia are less responsive and unable to maintain an overactivated state [56]. This includes reduced migration [57], clearance [58], neurotrophic factor release [59], and problems in changing from a pro-inflammatory to an anti-inflammatory state [60]. It might also be possible that in our model, microglia from adult mice are less reactive and incapable of protecting DA terminals from the early α-synuclein spreading. Further investigations are needed to understand if the reduction of DA terminals in the striatum is caused directly by microglial activation or vice versa. However, our results might suggest the existence of a compensatory mechanism involving structural adjustment of type B DA terminals affected by aggregate spreading and associated with a prompted microglia response during the early phase of anterograde α-synuclein spreading from SNpc. Adult DA neurons might have a less reactive structural adaptation, allowing a more prolonged harmful effect of α-synuclein spreading.

In conclusion, our study addressed the effect of α-synuclein PFFs inoculation in the nigrostriatal pathway, and the relationship between spreading of α-synuclein pathology, microglia reactivity, and neurotransmission (Figure 7). In our model, DA neurons from adult mice show more severe pathology in response to α-synuclein seeding and spreading along with the nigrostriatal pathway accompanied with reduced α-synuclein pathology in the midbrain, impaired neurotransmission, less reactive axonal adaptation, and less prominent microglial

activation compared with DA neurons of young animals. Our work suggests a new potential mechanism where compensatory pruning of large-sized DA terminals acts as an adaptive mechanism that guarantees normal DA release in the early stage of α-synuclein pathology in the striatum. Moreover, it supports the hypothesis that promoting rejuvenation of the microglia population might be important to protect dopaminergic neurotransmission during the early stage of α-synuclein spreading and influences the onset and progression of PD [61]. Also, future PFFs seeding studies need to carefully consider the age dependency of α-synuclein-induced effects in neurons to interpret and compare the data correctly, especially on the dopaminergic system.

ACKNOWLEDGMENTS

This work was funded by the Deutsche Forschungsgemeinschaft (DFG, German Research Foundation) under Germany's Excellence Strategy within the framework of the Munich Cluster for Systems Neurology—EXC 2145 SyNergy—ID 390857198 and the Marie Skłodowska-Curie Innovative Training Network (MSCA-ITN) “Synaptic Dysfunction in Neurodegenerative Diseases (SynDegen; EU Horizon 2020 AMD-721802-6). We thank the China Scholarship Council for the State Scholarship Fund (grant number 201606170111). We also thank Dr. Gerda Mitteregger, Dr. Meike Miller, Dr. Manuela Schneider, Dr. Anne von Thaden, Nadine Lachner, Elsa Clinton, and Mochen Cui for their excellent technical support.

CONFLICT OF INTEREST

The authors declare that they have no conflict of interest.

AUTHOR CONTRIBUTIONS

F.S., S.F., J.H., and C.S. conceived the research and designed the experiments. F.S. and S.B. performed PFFs preparation and surgery. F.S. performed FSCV experiments. F.S. and J.M.L. performed immunohistochemistry and confocal acquisition. F.S. and C.S. analyzed data. F.S., A.G.S., and C.S. wrote the manuscript. All authors edited and approved the final manuscript.

DATA AVAILABILITY STATEMENT

Data available on request.

ORCID

Carmelo Sgobio  <https://orcid.org/0000-0002-6282-369X>

REFERENCES

- Recasens A, Dehay B. Alpha-synuclein spreading in Parkinson's disease. *Front Neuroanat*. 2014;8:159.
- De Lau LM, Breteler MM. Epidemiology of Parkinson's disease. *Lancet Neurol*. 2006;5(6):525–35.
- Alegre-Abarrategui J, Brimblecombe KR, Roberts RF, Velentza-Almpani E, Tilley BS, Bengoa-Vergniory N, et al. Selective vulnerability in alpha-synucleinopathies. *Acta Neuropathol*. 2019;138(5):681–704.
- Luk KC, Kehm V, Carroll J, Zhang B, O'Brien P, Trojanowski JQ, et al. Pathological alpha-synuclein transmission initiates Parkinson-like neurodegeneration in nontransgenic mice. *Science*. 2012;338(6109):949–53.
- Luk KC, Kehm VM, Zhang B, O'Brien P, Trojanowski JQ, Lee VM. Intracerebral inoculation of pathological alpha-synuclein initiates a rapidly progressive neurodegenerative alpha-synucleinopathy in mice. *J Exp Med*. 2012;209(5):975–86.
- Luk KC, Song C, O'Brien P, Stieber A, Branch JR, Brunden KR, et al. Exogenous α -synuclein fibrils seed the formation of Lewy body-like intracellular inclusions in cultured cells. *Proc Natl Acad Sci USA*. 2009;106(47):20051–6.
- Volpicelli-Daley LA, Luk KC, Patel TP, Tanik SA, Riddle DM, Stieber A, et al. Exogenous alpha-synuclein fibrils induce Lewy body pathology leading to synaptic dysfunction and neuron death. *Neuron*. 2011;72(1):57–71.
- Henrich MT, Geibl FF, Lakshminarasimhan H, Stegmann A, Giasson BI, Mao X, et al. Determinants of seeding and spreading of alpha-synuclein pathology in the brain. *Sci Adv*. 2020;6(46):eabc2487.
- Hornykiewicz O. The discovery of dopamine deficiency in the parkinsonian brain. *J Neural Transm Suppl*. 2006;70:9–15.
- Collier TJ, Kanaan NM, Kordower JH. Ageing as a primary risk factor for Parkinson's disease: evidence from studies of non-human primates. *Nat Rev Neurosci*. 2011;12(6):359–66.
- Haycock JW, Becker L, Ang L, Furukawa Y, Hornykiewicz O, Kish SJ. Marked disparity between age-related changes in dopamine and other presynaptic dopaminergic markers in human striatum. *J Neurochem*. 2003;87(3):574–85.
- Le W, Wu J, Tang Y. Protective microglia and their regulation in Parkinson's disease. *Front Mol Neurosci*. 2016;9:89.
- Lindeberg J, Usoskin D, Bengtsson H, Gustafsson A, Kylberg A, Soderstrom S, et al. Transgenic expression of Cre recombinase from the tyrosine hydroxylase locus. *Genesis*. 2004;40(2):67–73.
- Blumenstock S, Rodrigues EF, Peters F, Blazquez-Llorca L, Schmidt F, Giese A, et al. Seeding and transgenic overexpression of alpha-synuclein triggers dendritic spine pathology in the neocortex. *EMBO Mol Med*. 2017;9(5):716–31.
- Kostka M, Högen T, Danzer KM, Levin J, Habeck M, Wirth A, et al. Single particle characterization of iron-induced pore-forming α -synuclein oligomers. *J Biol Chem*. 2008;283(16):10992–1003.
- Nuscher B, Kamp F, Mehnert T, Odoj S, Haass C, Kahle PJ, et al. α -Synuclein has a high affinity for packing defects in a bilayer membrane a thermodynamics study. *J Biol Chem*. 2004;279(21):21966–75.
- Conway KA, Lee S-J, Rochet J-C, Ding TT, Williamson RE, Lansbury PT. Acceleration of oligomerization, not fibrillization, is a shared property of both α -synuclein mutations linked to early-onset Parkinson's disease: implications for pathogenesis and therapy. *Proc Natl Acad Sci USA*. 2000;97(2):571–6.
- Deeg AA, Reiner AM, Schmidt F, Schueder F, Ryazanov S, Ruf VC, et al. Anle138b and related compounds are aggregation specific fluorescence markers and reveal high affinity binding to α -synuclein aggregates. *Biochim Biophys Acta*. 2015;1850(9):1884–90.
- Paxinos G, Franklin KB. Paxinos and Franklin's the mouse brain in stereotaxic coordinates. London: Academic Press; 2019.
- Sgobio C, Kupferschmidt DA, Cui G, Sun L, Li Z, Cai H, et al. Optogenetic measurement of presynaptic calcium transients using conditional genetically encoded calcium indicator expression in dopaminergic neurons. *PLoS One*. 2014;9(10):e111749.
- Sgobio C, Wu J, Zheng W, Chen X, Pan J, Salinas AG, et al. Aldehyde dehydrogenase 1-positive nigrostriatal dopaminergic fibers exhibit distinct projection pattern and dopamine release dynamics at mouse dorsal striatum. *Sci Rep*. 2017;7(1):5283.
- Yorgason JT, España RA, Jones SR. Demon voltammetry and analysis software: analysis of cocaine-induced alterations in dopamine signaling using multiple kinetic measures. *J Neurosci Methods*. 2011;202(2):158–64.
- Franklin KBJ, Paxinos G. The mouse brain in stereotaxic coordinates. San Diego: Academic Press; 2001.
- Luk KC, Covell DJ, Kehm VM, Zhang B, Song IY, Byrne MD, et al. Molecular and biological compatibility with host alpha-synuclein influences fibril pathogenicity. *Cell Rep*. 2016;16(12):3373–87.
- Masuda-Suzukake M, Nonaka T, Hosokawa M, Oikawa T, Arai T, Akiyama H, et al. Prion-like spreading of pathological alpha-synuclein in brain. *Brain*. 2013;136(Pt 4):1128–38.
- Fares M-B, Maco B, Oueslati A, Rockenstein E, Ninkina N, Buchman VL, et al. Induction of de novo α -synuclein fibrillization in a neuronal model for Parkinson's disease. *Proc Natl Acad Sci U S A*. 2016;113(7):E912–21.
- Butler B, Saha K, Rana T, Becker JP, Sambo D, Davari P, et al. Dopamine transporter activity is modulated by α -synuclein. *J Biol Chem*. 2015;290(49):29542–54.
- Chadchankar H, Ihalainen J, Tanila H, Yavich L. Decreased reuptake of dopamine in the dorsal striatum in the absence of alpha-synuclein. *Brain Res*. 2011;1382:37–44.
- Swant J, Goodwin JS, North A, Ali AA, Gamble-George J, Chirwa S, et al. α -Synuclein stimulates a dopamine transporter-dependent chloride current and modulates the activity of the transporter. *J Biol Chem*. 2011;286(51):43933–43.
- Arkadir D, Bergman H, Fahn S. Redundant dopaminergic activity may enable compensatory axonal sprouting in Parkinson disease. *Neurology*. 2014;82(12):1093–8.
- Gerfen CR, Staines WA, Arbuthnott GW, Fibiger HC. Crossed connections of the substantia nigra in the rat. *J Comp Neurol*. 1982;207(3):283–303.
- Veening JG, Cornelissen FM, Lieven PA. The topical organization of the afferents to the caudatoputamen of the rat. A horseradish peroxidase study. *Neuroscience*. 1980;5(7):1253–68.
- Braak H, Del Tredici K, Rüb U, De Vos RA, Steur ENJ, Braak E. Staging of brain pathology related to sporadic Parkinson's disease. *Neurobiol Aging*. 2003;24(2):197–211.

34. Janezic S, Threlfell S, Dodson PD, Dowie MJ, Taylor TN, Potgieter D, et al. Deficits in dopaminergic transmission precede neuron loss and dysfunction in a new Parkinson model. *Proc Natl Acad Sci U S A*. 2013;110(42):E4016–25.
35. Sgobio C, Sun L, Ding J, Herms J, Lovinger DM, Cai H. Unbalanced calcium channel activity underlies selective vulnerability of nigrostriatal dopaminergic terminals in Parkinsonian mice. *Sci Rep*. 2019;9(1):4857.
36. Del Tredici K, Braak H. Dysfunction of the locus coeruleus-norepinephrine system and related circuitry in Parkinson's disease-related dementia. *J Neurol Neurosurg Psychiatry*. 2013;84(7):774–83.
37. Gomez-Tortosa E, Sanders JL, Newell K, Hyman BT. Cortical neurons expressing calcium binding proteins are spared in dementia with Lewy bodies. *Acta Neuropathol*. 2001;101(1):36–42.
38. Seidel K, Mahlke J, Siswanto S, Kruger R, Heinsen H, Auburger G, et al. The brainstem pathologies of Parkinson's disease and dementia with Lewy bodies. *Brain Pathol*. 2015;25(2):121–35.
39. Spillantini MG, Crowther RA, Jakes R, Hasegawa M, Goedert M. α-Synuclein in filamentous inclusions of Lewy bodies from Parkinson's disease and dementia with Lewy bodies. *Proc Natl Acad Sci U S A*. 1998;95(11):6469–73.
40. Taguchi K, Watanabe Y, Tsujimura A, Tanaka M. Expression of alpha-synuclein is regulated in a neuronal cell type-dependent manner. *Anat Sci Int*. 2019;94(1):11–22.
41. Deniau JM, Mailly P, Maurice N, Charpier S. The pars reticulata of the substantia nigra: a window to basal ganglia output. *Prog Brain Res*. 2007;160:151–72.
42. Bendor JT, Logan TP, Edwards RH. The function of alpha-synuclein. *Neuron*. 2013;79(6):1044–66.
43. Larson ME, Greimel SJ, Amar F, LaCroix M, Boyle G, Sherman MA, et al. Selective lowering of synapsins induced by oligomeric alpha-synuclein exacerbates memory deficits. *Proc Natl Acad Sci U S A*. 2017;114(23):E4648–57.
44. Kiechle M, von Einem B, Hofs L, Voehringer P, Grozdanov V, Markx D, et al. In vivo protein complementation demonstrates presynaptic alpha-synuclein oligomerization and age-dependent accumulation of 8–16-mer oligomer species. *Cell Rep*. 2019;29(9):2862–74 e9.
45. Bernheimer H, Birkmayer W, Hornykiewicz O, Jellinger K, Seitelberger F. Brain dopamine and the syndromes of Parkinson and Huntington Clinical, morphological and neurochemical correlations. *J Neurol Sci*. 1973;20(4):415–55.
46. Fearnley JM, Lees AJ. Ageing and Parkinson's disease: substantia nigra regional selectivity. *Brain*. 1991;114(5):2283–301.
47. Chung SJ, Lee JJ, Lee PH, Sohn YH. Emerging concepts of motor reserve in Parkinson's disease. *J Mov Disord*. 2020;13(3):171–84.
48. Pettigrew C, Soldan A. Defining cognitive reserve and implications for cognitive aging. *Curr Neurol Neurosci Rep*. 2019;19(1):1.
49. Bolam JP, Pissadaki EK. Living on the edge with too many mouths to feed: why dopamine neurons die. *Mov Disord*. 2012;27(12):1478–83.
50. Matsuda W, Furuta T, Nakamura KC, Hioki H, Fujiyama F, Arai R, et al. Single nigrostriatal dopaminergic neurons form widely spread and highly dense axonal arborizations in the neostriatum. *J Neurosci*. 2009;29(2):444–53.
51. Liu C, Goel P, Kaeser PS. Spatial and temporal scales of dopamine transmission. *Nat Rev Neurosci*. 2021;22(6):345–58.
52. Rice ME, Cragg SJ. Dopamine spillover after quantal release: rethinking dopamine transmission in the nigrostriatal pathway. *Brain Res Rev*. 2008;58(2):303–13.
53. Pereira DB, Schmitz Y, Meszaros J, Merchant P, Hu G, Li S, et al. Fluorescent false neurotransmitter reveals functionally silent dopamine vesicle clusters in the striatum. *Nat Neurosci*. 2016;19(4):578–86.
54. Gerfen CR, Herkenham M, Thibault J. The neostriatal mosaic: II. Patch-and matrix-directed mesostriatal dopaminergic and non-dopaminergic systems. *J Neurosci*. 1987;7(12):3915–34.
55. Liu G, Yu J, Ding J, Xie C, Sun L, Rudenko I, et al. Aldehyde dehydrogenase 1 defines and protects a nigrostriatal dopaminergic neuron subpopulation. *J Clin Invest*. 2014;124(7):3032–46.
56. Caldeira C, Oliveira AF, Cunha C, Vaz AR, Falcao AS, Fernandes A, et al. Microglia change from a reactive to an age-like phenotype with the time in culture. *Front Cell Neurosci*. 2014;8:152.
57. Damani MR, Zhao L, Fontainhas AM, Amaral J, Fariss RN, Wong WT. Age-related alterations in the dynamic behavior of microglia. *Aging Cell*. 2011;10(2):263–76.
58. Li W. Phagocyte dysfunction, tissue aging and degeneration. *Ageing Res Rev*. 2013;12(4):1005–12.
59. Ma W, Cojocaru R, Gotoh N, Gieser L, Villasmil R, Cogliati T, et al. Gene expression changes in aging retinal microglia: relationship to microglial support functions and regulation of activation. *Neurobiol Aging*. 2013;34(10):2310–21.
60. Norden DM, Godbout JP. Review: microglia of the aged brain: primed to be activated and resistant to regulation. *Neuropathol Appl Neurobiol*. 2013;39(1):19–34.
61. Rodriguez M, Rodriguez-Sabate C, Morales I, Sanchez A, Sabate M. Parkinson's disease as a result of aging. *Aging Cell*. 2015;14(3):293–308.

SUPPORTING INFORMATION

Additional supporting information may be found in the online version of the article at the publisher's website.

FIGURE S1 Representative images of immunohistochemistry staining in PBS-injected SNpc and striatum of young and adult mice. Confocal acquisition of tile scanned SNpc reconstruction (left, scale bar: 100 μm) and dorsolateral striatum (right, scale bars 20 μm) coronal area sections, Contralateral to the images showed in figure 2. Phospho-α-synuclein (pSyn) in green, Tyrosine Hydroxylase (TH) in magenta and respective merged images. (A) Young and (B) Adult brain areas, 1 m.p.i. (C) Young and (D) Adult brain areas, 2 m.p.i.

FIGURE S2 Spreading of alpha-synuclein from the SNpc did not reach the motor cortex 2 months after PFFs inoculation. Phospho-α-synuclein (pSyn) staining in primary motor cortex and striatum acquired from the same coronal slice in young and adult mice, 2 m.p.i.. Immunoreactivity of pSyn-positive aggregates was observed only in the striatum ipsilateral to the PFFs injection. This observation validates our experimental design that use the contralateral hemisphere as internal control. Scalebar 50 μm

FIGURE S3 Distribution of α-synuclein aggregate numbers from SNpc to striatum. Number of α-synuclein aggregates in SNpc and striatum of young mice at 1 m.p.i. (A) and 2 m.p.i. (B), and in adult mice at 1 m.p.i. (C) and 2 m.p.i. (D). The number of aggregates in striata of young mice was significantly lower compared to adult mice (MANOVA significance in SNpc. Main Factor Treatment: $F(1) = 66.96$, $**p < 0.001$. MANOVA significance in the striatum. Interaction Treatment × Age × Anteroposteriorly: $F_{(1, 2)} = 4.9$, $*p < 0.05$; Interaction Treatment × Age × Seeding Time: $F_{(1, 1)} = 6.9$, $p < 0.05$. In the figures, LSD test: $###p < 0.001$ for comparison between different inoculation of same age; $***p < 0.001$ for

comparison between different age of same inoculation time). $n = 5$ mice per group, 3 technical repetitions for SNpc and 9 for striatum per hemisphere in each animal.

FIGURE S4 Increased microglial reactivity but no sign of astrogliosis in SNpc in mice 2 months after PFFs hemilateral injection. Pilot study where post-fixed mid-brain coronal sections from two seeded brains harvested for ex vivo FSCV experiments were used. (A) Raw data view in IMARIS software for of TH, GFAP and IBA1 (in red, left column) tdTomato reporter (in cyan blue) and phospho-alpha-synuclein (in green) and respective 3d reconstructions of SNpc (right column). Compared with dense IBA1 immunoreactivity within the SNpc, GFAP immunoreactivity was low and limited to the edges of the SNpc. Preliminary quantification of volumes covered by GFAP- (A) and IBA1- (B) positive signals in the SNpc after PFFs inoculation. We observed a trend of increasing microglial coverage between 1 and 2 m.p.i. in the seeded side, but an opposite, decreasing trend for the percentage area covered by reactive astrocytes. It is very likely that the reactivity of the microglia starts earlier

than the astrogliosis in response of alpha-synuclein spreading in the midbrain. Grid and Scalebar 25 μm

FIGURE S5 No sign of evident astrogliosis along nigrostriatal pathway in mice 2 months after PFFs hemilateral injection. Representative confocal acquisition of SNpc (A, average of stack image from volume of $212.34 \times 212.34 \times 43 \mu\text{m}$) and striatum (B, $212.34 \times 212.34 \times 49 \mu\text{m}$) from 5-month-old mouse showing GFAP (in Ceylon blue), Tyrosine Hydroxylase (TH) and Nissl (in magenta) immunoreactivity, 2 m.p.i.. In both area, astrocytes express very low level of GFAP protein, comparably in both seeded and not seeded area. Scale bars 20 μm

How to cite this article: Sun F, Salinas AG, Filser S, Blumenstock S, Medina-Luque J, Herms J, et al. Impact of α -synuclein spreading on the nigrostriatal dopaminergic pathway depends on the onset of the pathology. *Brain Pathol.* 2022;32:e13036. <https://doi.org/10.1111/bpa.13036>